SPLIT PHASE PROCESSING FOR ULTRASOUND SPECKLE REDUCTION: SIMULATED AND REAL DATA COMPARATIVE RESULTS

R.G. Dantas[1], E.T. Costa[2], S. Leeman[3]
[1,2]UNICAMP - FEEC/DEB/CEB, Campinas/SP, BRAZIL
[3]King's College London, London, UK
grossi@ceb.unicamp.br

Abstract

B-mode ultrasound images are characterised by the speckle artefact, which introduces fine-false structures whose apparent resolution is beyond the imaging system capabilities. Two widely used methods destined for speckle reduction are: a) split spectrum processing (SSP), and b) angular compounding. The first one is responsible for a significant resolution loss introduced in the final image. The second method requires a set of images scanned from different directions - a critical limitation in medical practice. Here, we propose a new speckle reduction technique that tackles the problem adjoining the characteristics of both angular compounding and SSP methods, but without their drawbacks. We have called it 'Split Phase Processing' (SPP) because it processes 2D data by using 2D directive filters to split the RF ultrasound image into a set of wide-band images with different phases. The outcomes of applying SPP to images generated by simulated and real laboratory acquired ultrasound pulses are shown.

Introduction

B-mode ultrasound images, as widely used for medical scanning, are characterised by the speckle artefact which results from interference effects between returning echoes, introducing false 'worm-like' structures whose resolution is beyond the ultrasound system capabilities, masking the true interfaces [1]. Two well-known methods developed for speckle reduction are Split Spectrum Processing (SSP), also known as frequency diversity, which is a single image technique, and Angular-, or Spatial-, Compounding (a multi-image method). The SSP output traditionally exhibits a significant resolution loss [2]. The angular compounding method [3] does not suffer from this problem but requires that the analysed structure be imaged from a number of different scanning directions - a severe practical limitation for medical imaging in particular.

The method proposed here may be seen as remedying the drawbacks of the two above techniques: it essentially maintains image resolution but requires only a single image as input. We have called the method 'Split Phase Processing' (SPP) because it processes image data by using two dimensional (2D) directive filters in frequency domain to split the RF ultrasound image into a set of relatively wide-band 'pre-images' with the same spectral amplitude components but with different (Fourier) phase functions.

Material and methods

SSP (Split Spectrum Processing) is a widely used single image technique originally developed for radar imaging systems. After single line data are stored, the 1D-backscattered signals (RF line) are split into different frequency bands through a set of narrow band-pass filters [4]. The filter outputs are envelope detected, weighted and compounded according to some rule (we have used the average of the normalised envelopes) in order to generate a 'speckle-reduced' image line (A-line). Relying on the idea that the backscattered signals emanating from structures are shown consistently in all frequency bands (within the pulse bandwidth limits), whilst the speckle pattern (being more noise-like) will be erratically different, the compounding of all bands hopefully lead to a structure enhancement and speckle reduction. However, the use of narrow-band filters implies that the final compounded signal will be more time-stretched (lower resolution) than the original one. In this sense, there is, strictly speaking, a trade-off between speckle reduction and resolution loss.

The angular compounding method does not suffer from this resolution loss limitation but it requires that the analysed structure be imaged from a number of different scanning directions. After that, all these images are compounded, generating an output with reduced speckle interference. The best results are obtained with a full 180° range - a severe practical limitation for medical imaging in particular. Another disadvantage relies on the fact that the final image is available only after the acquisition of the last image, meaning that this method cannot be used in real time.

We were aiming a speckle reduction method that could overcome the drawbacks of these two later methods: a single image one (unlike angular compounding) with no resolution loss (unlike SSP). The method we have introduced is schematically illustrated in figure 1. The 2D RF image, x (m,n), is split by a set of 2D wide-band filters. After the envelope detection stage, the filter outputs are weighted/normalised and compounded back into a 'speckle-reduced' image. The speckle decorrelation was achieved by using directive wide-band filters, applied at different directions in 2D frequency domain. Each such filter outputs a different interference pattern (speckle) while leaving the structure relatively intact. Hence, a wide-band filtering at different directions is able to decorrelate the speckle while keeping the image's original resolution.

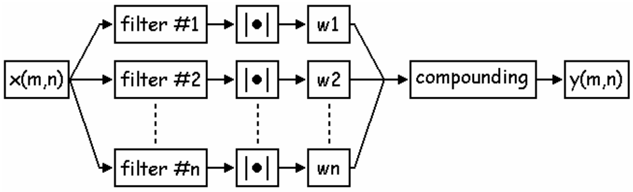

Figure 1 – 2D SPP basic scheme showing the input RF image, x(m,n), the wide-band filters, the envelope detection, weighting and compounding stage, resulting in the speckle-reduced image y(m,n).

Radial Gaussian filters (truncated at –40dB) have been used, with examples shown in figure 2: a single filter on the left-hand side and a set of 7 superimposed filters on the right. The use of directive filters makes the new technique a 'phase diversity' method, hence the designation: split phase processing, 'SPP'. The bandwidth of a single filter is chosen to be close to that of the ultrasound pulse, because the latter essentially determines the image bandwidth, and, hence, its resolution. In the present case, the axial and lateral bandwidths are the same but the filter shape can be asymmetric, suiting the RF image spectrum. Its radius corresponds to the pulse central frequency.

As each filter outputs a 'pre-image' with a different brightness, the normalisation becomes an important stage, providing the same 'strength' for all pre-images. They were normalised by area, meaning that the sum of all pixel values for each image is equal to 1.

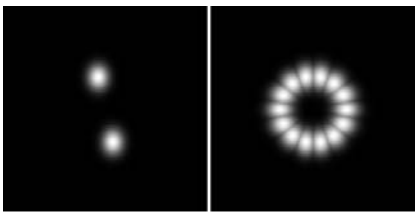

Figure 2 – Example of 2D directive radial filters used in the 2D SPP method. Left: one 2D directive Gaussian radial filter; right: superposition of 7 filters.

Probably, the most accurate way to analyse the performance of a speckle reduction method should be by visual inspection. However, in order to quantify the method's performance level, we have adopted the pooled signal to noise ratio (SNR) and contrast to noise ratio (CNR) between two different image regions, marked as (a) and (b) in figure 3. These indexes are calculated via the following equations [5]:

$$SNR = \frac{\mu_A + \mu_B}{2 \cdot \sqrt{\sigma_A^2 + \sigma_B^2}} \qquad (1)$$

$$CNR = \frac{|\mu_A - \mu_B|}{\sqrt{\sigma_A^2 + \sigma_B^2}} \qquad (2)$$

Even though SNR and CNR are such widely used image quality parameters, they do not include any measurement of the resolution loss. Another quality parameter is the texture analysis, calculated as the overlapping width of the foreground and background histograms. Figure 3.b shows both histograms of regions A (background) and B (foreground) of figure 3.a. As the image is fully speckle developed, the intersection between the two histograms is significant. In a speckle-free image the histogram overlapping would be minimum. The histogram width is calculated at 50% of the peak of the intersected area (marked by an arrow).

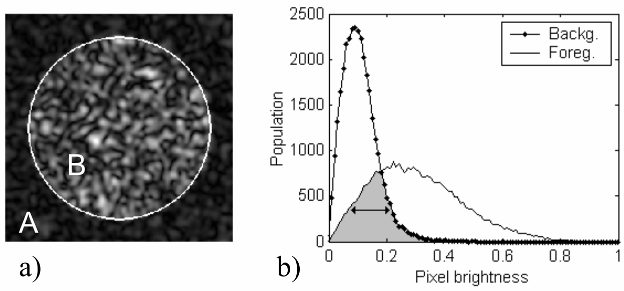

a) b)

Figure 3 – B-mode image showing the regions of interest (A and B) where the SNR and CNR were calculated.

Results

The phantom used to generate the simulated B-mode image is made with complex point scatterers distributed with random position, magnitude and phase. The 'structure' is distinguished from the background by increasing the scatterers mean magnitude by the factor of 3. We used three different ultrasound pulses: a simulated one and two real laboratory acquired ones. The simulated pulse has a gaussian-like shape, truncated at –20dB of is peak, bandwidth of 50%, central frequency of 3.0MHz and sampling rate of 18MHz. The real pulses were acquired in a water tank. The first one was generated by a 2.25 MHz transducer (Funbec, non-focused, 13 mm diameter, model 166173H), in the far filed, at 50 mm from its face. After digitalization it was decimated to 50x50 pixels size. The second pulse was generated by a 1.00 MHz transducer (Panametrics, focused at 15.3 mm from its faced), in the focal zone, and decimated to 40x40 pixels. The transducers were fired by short-time high energy pulses from a Panametrics pulser/receiver (model 5072PR) and detected by a 0.30 mm diameter ceramic point hydrophone (J. Weight, City University, London, UK) and acquired on a PC-type computer from a digital oscilloscope (Tektronix 2430A) with a GPIB interface. The pulses were laterally scanned with a 0.10 mm resolution.

Even thought we have used both simulated and real pulses, the use of simulated phantom is appropriate at this stage because it provides the possibility of calculating the speckle-free image: i.e., where the scatterers' phase may be changed directly in order to achieve only constructive interference. The construction of such a 'golden standard' image is clearly not possible with real images, where the scattering structures, and their phases, are unknown. It is generated artificially by constraining all the interference to be constructive, via the convolution of the pulse envelope with the magnitude of the point scatterers [6].

Figure 4 shows the three used pulses: the simulated one (fig. 4.a), the non-focused one (fig. 4.b) and the focused one (fig. 4.c). Figures 5 to 9 correspond to results that are organised, from left to right, to images derived from the pulses shown in figure 4. Figure 5 shows the resultant B-mode images obtained with the three later described pulses with the same simulated phantom. The fine 'worm-like' structures snaking through the image are a direct consequence of the interference effects that give rise to the speckle artefact, pervading the entire image wherever interference can occur. The speckle-free images are shown in figure 6. These images indicate the best that a speckle-reduction technique can achieve; any grey-scale variations are due to local fluctuations in the mean scatterer strength, and not interference.

Figure 7 shows the outputs of the conventional line-by-line SSP method, with five 1D filters (55% overlapping) chosen and envelope average, as the compounding rule. Because of the choice of pulse, the individual A-lines making up the image run horizontally. Some deep minima are still present, indicating that the speckle reduction is far from being optimal. More complete speckle reduction is achievable by choosing more and narrower filters, resulting, however, in even more resolution loss than that already evident. Figure 8 shows the outputs of the angular compounding method, representing the average of 7 images obtained at equal angular intervals (10°) over a 60° viewing range (which we regard as a practicable upper limit in most medical applications, although best results are obtained with a full 180° range).

Figure 9 shows the 7 directive filters used in each case. For visual purpose only, a pair of them was highlighted. As can be seen, the radius as well as the axial and lateral bandwidths changes according to the pulses. Figure 10 shows the output of Split Phase Processing: it clearly represents an improvement over conventional SSP, both in terms of approximation to the speckle-free image, as well as retention of the original resolution. Also, the edges of the object appear to be sharper. In terms of speckle reduction level and resolution loss, this result is comparable to the angular compounding one, but is achieved with only a single image.

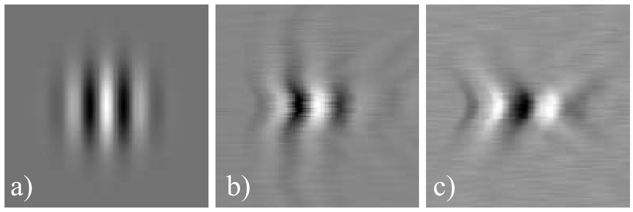

Figure 4 – a) Simulated pulse, non-focused 2.25 MHz pulse (Funbec) and c) focused 1.00 MHz pulse (Panametrics).

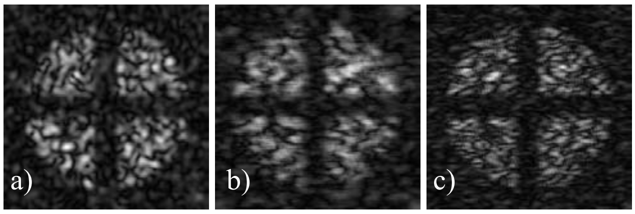

Figure 5 – B-mode images obtained with the pulses shown in figure 4.

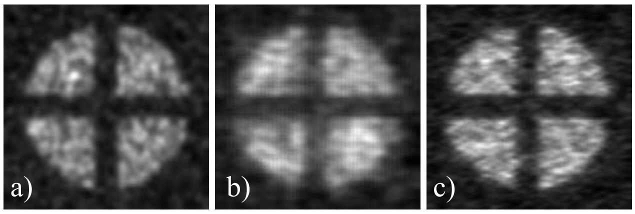

Figure 6 – Speckle-free images of figures 5.a to 5.c.

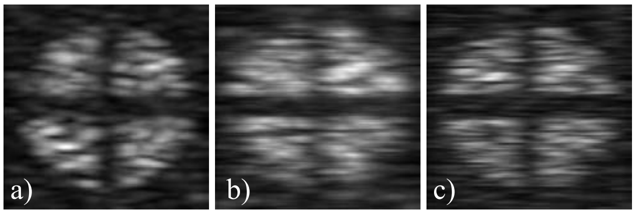

Figure 7 – SSP outputs of images 5.a to 5.c.

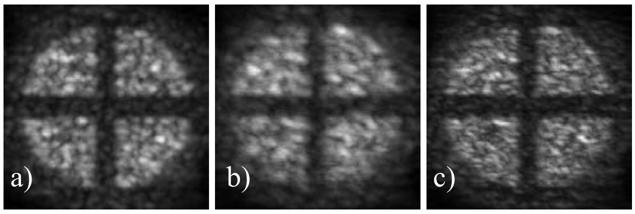

Figure 8 – Angular compounding outputs of images 5.a to 5.c.

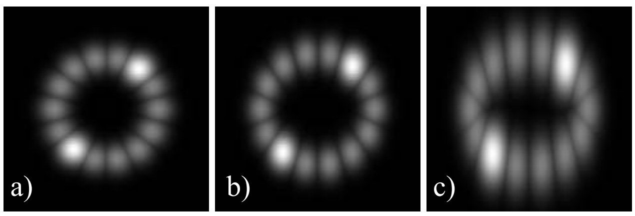

Figure 9 – Directive filters used with the RF images which envelopes are shown in figure 5 (a pair of filter is highlighted in each image for visual purpose only).

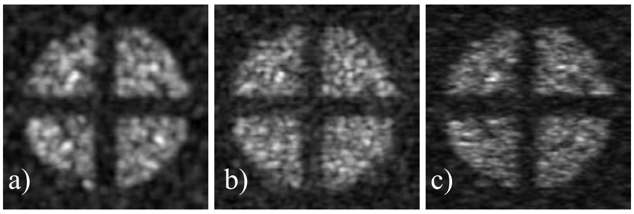

Figure 10 – SPP outputs of images 5.a to 5.c.

The performances of the different speckle reduction methods were quantitatively judged, in terms of SNR, CNR and histogram width, with respect to a two-region phantom, with a sample B-mode image shown in figure 3. The two regions of interest (ROI) A and B have the same dimensions, whilst the image size is 256 x 256 pixels. These quality parameters were calculated for a 20 different image set, and their averages, with 1 standard deviation, are summarised in table 1, 2 and 3 (relative to B-mode image), brought about by the methods described above. The numerical results appear to closely agree with the impressions of a visual inspection of the images. The acronyms BM, SF, SSP, AC and SPP correspond, respectively, to B-mode image, speckle-free image, SSP output, angular compounding output and SPP output.

Table 1 – Relative average SNR*, CNR* and histogram width* of 20 sets of images with the simulated pulse (*relative to B-mode).

Image	SNR*	CNR*	Hist. width*
BM	1	1	1
SF	2.09 ± 0.090	2.78 ± 0.113	0.13 ± 0.016
SSP	1.34 ± 0.056	1.38 ± 0.068	0.59 ± 0.063
AC	1.60 ± 0.038	1.62 ± 0.060	0.44 ± 0.029
SPP	1.78 ± 0.068	1.96 ± 0.094	0.27 ± 0.025

Table 2 – Relative average SNR*, CNR* and histogram width* of 20 sets of images with the Funbec 2.25 MHz pulse (*relative to B-mode).

Image	SNR*	CNR*	Hist. width*
BM	1	1	1
SF	1.97 ± 0.066	2.33 ± 0.066	0.18 ± 0.016
SSP	1.54 ± 0.050	1.63 ± 0.045	0.44 ± 0.035
AC	1.46 ± 0.043	1.47 ± 0.038	0.51 ± 0.024
SPP	1.79 ± 0.061	2.06 ± 0.062	0.25 ± 0.019

Table 3 – Relative average SNR*, CNR* and histogram width* of 20 sets of images with the Panametrics 1.00 MHz pulse (*relative to B-mode).

Image	SNR*	CNR*	Hist. width*
BM	1	1	1
SF	2.02 ± 0.123	2.43 ± 0.091	0.20 ± 0.019
SSP	1.43 ± 0.059	1.47 ± 0.072	0.57 ± 0.056
AC	1.54 ± 0.058	1.55 ± 0.054	0.48 ± 0.028
SPP	1.90 ± 0.090	2.23 ± 0.099	0.27 ± 0.027

Discussion and conclusion

The traditional 1D SSP method presents a relatively high-resolution loss limitation, inherent to the method, impinging a strictly trade-off between the speckle reduction level and the resolution loss. On the other hand, the new 2D SPP with directive filters does not present a noticeable resolution loss, voiding the conventional method's drawback. The fact that these filters have their spectra wider than the ultrasound pulse spectrum helps to keep the image's original resolution.

The use of directive filters in the SPP method has a similarity with the angle compounding method, because the first decorrelates speckle by filtering the image at different angles, whilst the later uses images acquired from different angles. However, the angle compounding method has a practical limitation due to the difficulty in acquiring images from certain angles, besides the fact that it is a multi-image method, whilst the SPP requires a single image only.

The quantitative analysis (tables 1, 2 and 3) agrees with visual inspection in the sense that the new SPP method is able to strongly perform speckle reduction while keeping edges details, without any noticeable resolution loss.

The filtering parameters, such as number of filter, bandwidth or superposition level, were determined empirically, in order to get the 'best' results. Otherwise, once these parameters were found, they can be kept unchanged and be used again for the same kind of ultrasound pulse, providing some robustness level to the method.

Acknowledgements

CAPES (Brazil) and FAPESP (Brazil) are gratefully acknowledged for the financial support.

References

[1] C.B. Burckhardt, "Speckle in Ultrasound B-Mode Scans", IEEE Trans. Sonics and Ultrasonics, vol. 25, n. 1, pp. 1-6, January, 1978.

[2] P.M. Shankar, V.L. Newhouse, "Speckle Reduction with Improved Resolution in Ultrasound Images", IEEE Trans. Sonics and Ultrasonics, vol. 32, n. 4, July, pp. 537-543, 1985.

[3] P.C. Li and M. O'Donnell, "Evaluational spatial compounding", Ultrasonic Imaging, vol. 16, 3, pp. 176-189, 1994.

[4] A.J. Healey, S. Leeman, L.A. Ferrari, "Removing the Ambiguity from Single Image Speckle Reduction Techniques", Acoustical Imaging, vol. 22, pp. 145-150, 1996.

[5] Y. Chen, R. Yin, P. Flynn, S. Broschat, "Aggressive region growing for speckle reduction in ultrasound images", Pattern Recognition Letters, vol. 24, 4-5, February, pp. 677-691, 2003.

[6] S.M. Gehlbach, "Pulse reflection imaging and acoustic speckle", Ph.D. dissertation, Stanford University, 1983.